arXiv:hep-ph/9611313v1 12 Nov 1996

McGill/96-41

Derivation of the Lamb Shift using an Effective Field Theory

Patrick Labelle [1]

Department of Physics, Bishop's University
Lennoxville, Québec, Canada J1M 1Z7

and

S. Mohammad Zebarjad[2]

Department of Physics, McGill University
Montréal, Québec, Canada H3A 2T8

Abstract

We rederive the $\mathcal{O}(\alpha^5)$ shift of the hydrogen levels in the non-recoil limit ($m_e/m_P \to 0$) using Nonrelativistic QED (NRQED), an effective field theory developed by Caswell and Lepage (Phys. Lett.**167B**, 437 (1986)). Our result contains the Lamb shift as a special case. Our calculation is far simpler than traditional approaches and has the advantage of being systematic. It also clearly illustrates the need to renormalize (or "match") the coefficients of the effective theory beyond tree level.

[1]labelle@hep.physics.mcgill.ca
[2]zebarjad@hep.physics.mcgill.ca

1 Introduction

The Lamb shift, the shift between the hydrogen $2S_{1/2}$ and $2P_{1/2}$ states, is without any doubt the most well-known bound state application of radiative corrections. It has the form $m_e\alpha^5(\ln\alpha + \text{finite})$ where the finite piece contains the Bethe logarithm, a state dependent term that must be evaluated numerically. The log term is relatively easy to extract and its calculation is presented in many quantum mechanics textbooks. The finite contribution is much more difficult to evaluate because it requires the application of QED to a bound state. In this paper, we rederive the complete $\mathcal{O}(\alpha^5)$ corrections in the non-recoil limit[1] ($m_e/m_P = 0$) using NRQED, an effective field theory developed by Caswell and Lepage [1], as extended by Labelle [2] to study retardation effects.

To construct NRQED, one writes down the most general Lagrangian consistent with the low energy symmetries of QED such as parity and gauge invariance, etc. The first few terms of this Lagrangian are given by (we follow the notation of [7])

$$\begin{aligned}\mathcal{L}_{2-Fermi} &= \psi^\dagger\{iD_t + \frac{\mathbf{D}^2}{2m} + \delta_R\frac{\mathbf{D}^4}{8m^3} + \delta_F\frac{q\boldsymbol{\sigma}\cdot\mathbf{B}}{2m} + \delta_D\frac{q(\mathbf{D}\cdot\mathbf{E} - \mathbf{E}\cdot\mathbf{D})}{8m^2} \\ &\quad + \delta_S\frac{iq\boldsymbol{\sigma}\cdot(\mathbf{D}\times\mathbf{E} - \mathbf{E}\times\mathbf{D})}{8m^2} + \ldots\}\psi_e \\ &\quad + \text{ same terms with } \psi_e \to \psi_p \ + \ \text{photon terms}, \end{aligned} \tag{1}$$

where ψ_e and ψ_p are two component fields associated with the electron and proton, respectively. There are of course many other interactions, including four-fermion interactions, however, as we will discuss below, those are not relevant at $\mathcal{O}(\alpha^5)$. For the photon, we use the Coulomb gauge which is the most efficient gauge to study nonrelativistic bound states since it permits to isolate the Coulomb interaction (which must be treated nonperturbatively) from all other interactions (which can be treated as perturbations). In that gauge, the photon terms in Eq.(1) are

$$-\frac{1}{4}F_{\mu\nu}F^{\mu\nu} + \delta_{VP}\frac{\alpha}{15\pi}A^0(\mathbf{k})\frac{\mathbf{k}^4}{m^2}A^0(\mathbf{k}) - \delta_{VP}\frac{\alpha}{15\pi}A^i(k)\frac{\mathbf{k}^4}{m^2}A^j(k)\ (\delta_{ij} - \frac{k_ik_j}{\mathbf{k}^2}) + \ldots \tag{2}$$

Using $\mathbf{D} = i(\mathbf{p} - q\mathbf{A})$ and $D_t = \partial_t + iqA_0$, the NRQED hamiltonian can be written as

$$\begin{aligned}\mathcal{H} = \psi'^\dagger\Big[\frac{\mathbf{p}^2}{2m} &+ qA_0 - \frac{\mathbf{p}^4}{8m^3} - \frac{q}{2m}(\mathbf{p}' + \mathbf{p})\cdot\mathbf{A} + \frac{q^2}{2m}\mathbf{A}\cdot\mathbf{A} \\ &-\delta_F\frac{iq}{2m}\boldsymbol{\sigma}\cdot(\mathbf{k}\times\mathbf{A}) - \delta_D\frac{q}{8m^2}\mathbf{k}^2A^0 + \delta_S\frac{iq}{4m^2}\boldsymbol{\sigma}\cdot(\mathbf{p}'\times\mathbf{p})A^0 \\ &+\delta_S\frac{iq}{8m^2}k^0\boldsymbol{\sigma}\cdot(\mathbf{p}' + \mathbf{p})\times\mathbf{A} - \delta_S\frac{iq}{4m^2}\boldsymbol{\sigma}\cdot(\mathbf{k}_1\times\mathbf{A}(k_1))A^0(k_2) + \ldots\Big]\psi, \end{aligned} \tag{3}$$

[1] In the literature, these corrections are also referred to as the Lamb shift. We will also adopt this notation in the rest of the paper.

and the photon hamiltonian can be written as

$$\mathcal{H}_{photon} = \frac{1}{2}(\mathbf{E}^2 + \mathbf{B}^2) - \delta_{VP}\frac{\alpha}{15\pi}A^0(\mathbf{k})\frac{\mathbf{k}^4}{m^2}A^0(\mathbf{k}) + \delta_{VP}\frac{\alpha}{15\pi}A^i(k)\frac{\mathbf{k}^4}{m^2}A^i(k)(\delta_{ij} - \frac{k_i k_j}{\mathbf{k}^2}) + \dots \tag{4}$$

The Feynman rules of Eqs.(3) and (4) are given in Fig.[1].

The photon propagator requires a special treatment. We use time-ordered perturbation theory (in which all particles are on-shell but energy is not conserved at the vertices) and, as mentioned above, we work in the Coulomb gauge. In a time-ordered diagram, Coulomb photons propagate instantaneously (*i.e.* along vertical lines in our diagrams since we choose the time axis to point to the right) and transverse photon propagate in the time direction. The corresponding Feynman rules are given in Figs.[2] and [3].

As is shown in [2], the power of NRQED is enhanced if one separates "soft" transverse photons (having energies of order $\gamma \equiv Z\mu\alpha$) from the "ultra-oft" photons (with $E \simeq \gamma^2/\mu$) because the counting rules differ for the two types of photons. In that reference, it is also shown that the multipole expansion can be applied to the vertices containing ultra-soft photons. The distinction between soft and ultra-soft photons is particularly important in this work because the Lamb shift involves both types of contributions. We have therefore separated the general photon propagator of Fig.[4] into a contribution corresponding to a soft photon, Fig.[4(a)], and the contribution corresponding to an ultra-soft photon, Fig.[(4b)].

Finally, in NRQED loop diagrams, all internal momenta must be integrated over, with a measure $d^3p/(2\pi)^3$.

The unknown coefficients $\delta_R, \delta_F \dots$ can be found by imposing that NRQED is equivalent to QED for nonrelativistic scattering processes, *i.e.* by imposing

$$\begin{array}{c}\text{NRQED scattering}\\ \text{amplitudes}\end{array} \quad = \quad \begin{array}{c}\text{QED scattering amplitudes}\\ \text{expanded in powers of } \mathbf{p}/m.\end{array}$$

This is the so-called matching procedure. Notice that no bound state physics enters at this stage of the calculation.

The coefficients appearing in (3) can be fixed by considering the scattering of an electron off an external field A_μ. This is illustrated, at tree level, in Fig.[5]. We have chosen the normalization of the interactions of Eq.(3) in such a way that the tree level matching gives $\delta = 1$ for all the coefficients appearing in (3). The first non-zero contribution to δ_{VP} comes from the one-loop QED vacuum polarization diagram, as illustrated in Fig.[6] and, again, our normalization is such that $\delta_{VP} = 1$, to one loop [7]. We will still refer to this as "tree level matching" because only tree level NRQED diagrams are involved (similarly, n-loops matching will refer to the number of loops "n" the NRQED diagrams). The one-loop matching will bring $\mathcal{O}(\alpha)$ corrections to the coefficients $\delta' s$.

We are now in position to proceed with the calculation. All NRQED calculations can be divided into three steps. The first one consists in using the counting rules to identify the

diagrams which will contribute to the order of interest. This first step not only permits to identify the relevant diagrams but it also fixes the order (in the number of loops) at which the coefficients must be matched. The second step consists in matching the coefficients to the order required and the last step corresponds to finally evaluating the NRQED bound state diagrams.

In our case, we first need to isolate the NRQED diagrams contributing to order α^5 in the non-recoil limit *i.e.* we neglect corrections suppressed by powers of m_e/m_p. As a simpler example, we will first isolate the diagrams contributing to order α^4 in the non-recoil limit (the full NRQED calculation of the $\mathcal{O}(\alpha^4)$ energy shift for arbitrary masses will be presented in Ref.[8]). In that limit, the only relevant diagrams are shown in Fig.[7]. This can easily be checked by using the NRQED counting rules derived in Ref.[2]. Since soft and ultra-soft photons obey different counting rules, we consider their contribution in turn. Soft photons contribute to order :

$$\frac{\mu^{\kappa+\rho+1}}{m_e^{\kappa} m_p^{\rho}} Z^{\eta} \alpha^{\zeta} \approx \frac{m_e^{\rho+1}}{m_p^{\rho}} \alpha^{\zeta}, \tag{5}$$

where μ is the reduced mass and ρ and κ are, respectively, the total number of inverse powers of m_p and m_e appearing in the NRQED vertices. In (5), we approximated $\mu \approx m_e$ which is exact in the non-recoil limit. The coefficient ζ is defined by

$$\zeta = 1 + \kappa + \rho - N_{TOP} + \sum_i n_i, \tag{6}$$

where N_{TOP} is the number of intermediate state time-ordered propagators (see Ref.[2] for more details) and last term is the sum of factors of α contained in the vertices (including possible factors coming from the δ's). Now, to obtain the correction of order $m_e\alpha^4$, we need to have $\rho = 0$ and $\zeta = 4$ (see Eq.(5)). The only way to have $\rho = 0$ is to either have a Coulomb interaction on the nucleus line or no interaction at all. This already reduces greatly the possible diagrams. Turning now to the condition $\zeta = 4$, we obtain from Eq.(6)

$$\kappa - N_{TOP} + \sum_i n_i = 3. \tag{7}$$

Since in first order of perturbation theory $N_{top} = 0$, we are left with the condition $\kappa + \sum_i n_i = 3$. One possibility is $\kappa = 3$ and $\sum n_i = 0$ which corresponds to the relativistic kinetic energy vertex on the electron line. Another possibility is $\kappa = 2$ and $\sum a_i = 1$ which can be fulfilled with the Coulomb vertex on the proton line and either the Darwin or the Spin-Orbit interaction on the electron line. There are no Coulomb interaction with only one inverse mass so the condition $\kappa = 1$ and $\sum n_i = 2$ cannot be satisfied. The three possible diagrams are illustrated in Fig.[7].

To order α^5, and still in first order of perturbation theory, we must either increase κ or $\sum n_i$ by one. It is not possible to increase the number of inverse electron masses κ by one, but there are two ways to increase $\sum n_i$ by one. One is to include the one-loop corrections to the coefficients δ's of the vertices in Fig.[7], so we will have to match these interactions

to one loop. The other possibility for $\kappa = 2$ and $\sum n_i = 2$ is to consider the new interaction corresponding to the vacuum polarization correction to the Coulomb propagator which is depicted in Fig.[8].

We now turn to diagrams in second order of perturbation theory, in which case $N_{TOP} = 1$. It can easily be verified that ζ, Eq.(6), cannot then be made equal to 5. We have now uncovered all the diagrams containing only soft photons which contribute to order α^5. The only remaining possibility is to consider diagrams with ultra-soft photons which lead to a contribution of the form given by Eq.(5) but now with (see Ref.[2]):

$$\zeta = \sum_i n_i + 1 + \rho + \kappa - N_{top} + 2N_\gamma + \sum_i \mathcal{M}_i, \tag{8}$$

where N_γ is the number of ultra-soft photons in the diagram and $\mathcal{M}_i$ is the order, in the multipole expansion, of the i_{th} vertex and the sum is over the vertices connected to ultra-soft photons only. As before, we set $\zeta = 5$ and $\rho = 0$ to obtain non-recoil corrections of order α^5. For diagrams containing ultra-soft photons, the minimum value of N_{TOP} is 1, because these photons propagate in the time direction (we again refer the reader to Ref.[2] for more details). Working at the zeroth order of the multipole expansion ($\mathcal{M}_i = 0$) and considering only one ultra-soft photon ($N_\gamma = 1$), we then have the condition $\kappa + \sum n_i = 3$. Since the ultra-soft photon is necessarily transverse and transverse vertices contain at least one power of inverse mass (see Fig.[1]), κ is bigger or equal to 2. In addition, $\sum n_i$ is at least equal to one (*i.e.* there at least a total number of one factor of α in the vertices). We therefore already fulfill the condition $\kappa + \sum n_i = 3$ with the simplest diagram which corresponds to an ultra-soft photon connected to two $\mathbf{p}\cdot\mathbf{A}$ vertices, as represented in Fig.[9].

We have now identified all diagrams contributing to the order of interest. We now turn to the matching. From the above discussion, we see that we need to match to one loop the coefficients of the interactions contributing to order α^4.

To make NRQED agree with QED at the one loop order, we impose the relation illustrated in Fig.[10]. This matching was performed in [7] but, even though our final result is of course the same, our derivation differs sufficiently to be presented it here. The QED scattering amplitude (the left hand side of Fig.[10]) can be expressed in terms of the usual form factors $F_1(Q^2)$ and $F_2(Q^2)$ in the following way (to be consistent, we use a nonrelativistic normalization for the Dirac spinors):

$$\begin{aligned}
&-e\frac{\bar{u}(\mathbf{p}\,',\mathbf{s}')}{\sqrt{2E'}}\Big[\gamma_0\, A^0(\mathbf{Q})F_1(Q^2) - \frac{i}{2m}\sigma^{0j}\, A^0(\mathbf{Q})\; Q^j\; F_2(Q^2)\Big]\,\frac{u(\mathbf{p},\mathbf{s})}{\sqrt{2E}} \quad = \\
&F_1(Q^2)\xi'^{\dagger}\Big[-eA^0 + \frac{e}{8m^2}\mathbf{Q}^{\,2}A^0 - \frac{ie}{4m^2}\boldsymbol{\sigma}\cdot(\mathbf{p}\,'\times\mathbf{p})A^0 + \ldots\Big]\xi + \\
&F_2(Q^2)\xi'^{\dagger}\Big[\frac{e}{4m^2}\mathbf{Q}^{\,2}A^0 - \frac{ie}{2m^2}\boldsymbol{\sigma}\cdot(\mathbf{p}\,'\times\mathbf{p})A^0 + \ldots\Big]\xi,
\end{aligned} \tag{9}$$

where $\mathbf{Q} = \mathbf{p}' - \mathbf{p}$, $\mathbf{s}$ and $\mathbf{s}'$ are the initial and final spin of the electron, respectively, and ξ, ξ' are the corresponding initial and final two component Pauli spinors normalized to

unity. We choose the convention that e is positive so that the charge of the electron is $-e$. In (9), as in the rest of the paper, we use m to represent the mass of the electron. Notice that the matching involves a double expansion. One expansion is in the coupling constant α and the other is the nonrelativistic expansion in $\mathbf{Q}/m$ which leads to renormalization of different NRQED operators. The nonrelativistic expansions of the form factors are [7]

$$\begin{aligned} F_1(Q^2) &= 1-\frac{\alpha}{3\pi}\Big[\frac{\mathbf{Q}^{\,2}}{m^2}\Big(\ln(\frac{m}{\lambda})-\frac{3}{8}\Big)\Big]+\dots \\ F_2(Q^2) &= a_e-\frac{\alpha}{\pi}\frac{\mathbf{Q}^{\,2}}{12m^2}+\dots . \end{aligned} \tag{10}$$

where a_e is the electron anomalous magnetic moment which, to the order of interest, can be taken to be $\alpha/(2\pi)$. In the above Eqs., since Q^0 is of order of v^2 and $|\mathbf{Q}|$ is of order v, we have ignored Q^0 respect to $\mathbf{Q}$.

If we substitute (10) in (9) we obtain

$$\begin{aligned} \xi'^{\dagger}\,(-eA^0)\,\xi \quad &+ \quad \frac{e}{8m^2}\xi'^{\dagger}\,\mathbf{Q}^2A^0\xi\Big[1+\frac{8\alpha}{3\pi}\Big(\ln(\frac{m}{\lambda})-\frac{3}{8}\Big)+2a_e+\dots\Big] \\ &\quad -\frac{ie}{4m^2}\xi'^{\dagger}\,\boldsymbol{\sigma}\cdot(\mathbf{p}'\times\mathbf{p})A^0\,\xi\Big[1+2a_e+\dots\Big]+\mathcal{O}(\mathbf{Q}^4/m^4). \end{aligned} \tag{11}$$

We must now compute the right-hand side of Fig.[10] to complete the calculation of the one-loop renormalized NRQED coefficients. Since we are dealing with ultra-soft photons in Figs. [10(h)], [10(i)] and [10(k)], we use the special Feynman rules derived in Ref.[2]. Working at the zeroth order of the multipole expansion, Fig.[10(h)] corresponds to

$$\begin{aligned} \xi'^{\dagger}(\frac{2ep_i}{2m})(\frac{2ep'_j}{2m}) \quad &\int\frac{d^3k}{(2\pi)^3}\frac{\delta_{ij}-\frac{k_ik_j}{\mathbf{k}^2+\lambda^2}}{2\sqrt{\mathbf{k}^2+\lambda^2}}\;\frac{1}{-\sqrt{\mathbf{k}^2+\lambda^2}}\;(-eA_0)\;\frac{1}{\frac{\mathbf{p}^2}{2m}-\frac{\mathbf{p}'^2}{2m}-\sqrt{\mathbf{k}^2+\lambda^2}}\;\xi \\ &\approx\; \xi'^{\dagger}(-eA_0)\xi\,(\frac{e}{m})^2\;\frac{\mathbf{p}'\cdot\mathbf{p}}{3}\int\frac{dk\;\mathbf{k}^2}{2\pi^2}\;\;\frac{2\mathbf{k}^2+3\lambda^3}{\mathbf{k}^2+\lambda^2}\;\;\frac{1}{2\sqrt{\mathbf{k}^2+\lambda^2}}\frac{1}{\mathbf{k}^2+\lambda^2} \\ &=\; -\frac{8\alpha}{3\pi}\Big[\ln(\frac{2\Lambda}{\lambda})-\frac{5}{6}\Big]\,\xi'^{\dagger}eA_0\xi\,\frac{\mathbf{p}\cdot\mathbf{p}'}{4m^2} \end{aligned} \tag{12}$$

where, in the second line, we have used the fact that the integral is already proportional to $\mathbf{p}\cdot\mathbf{p}'$ to approximate $\mathbf{p}^2\approx\mathbf{p}'^2\approx 0$ in the propagators. The corrections to these expressions will lead to higher order operators.

Notice that we are only working with scattering diagrams when performing the matching, no bound state physics enters this stage of the calculation. To compute the amplitudes in Figs.[10(i)] and [10(k)], we just need to evaluate the first one and then obtain the second one by replacing $\mathbf{p}$ by $\mathbf{p}'$. For Fig.[10(i)], we can write

$$\frac{1}{2}\xi'^{\dagger}(\frac{2ep_i}{2m})(\frac{2ep_j}{2m})\int\frac{d^3k}{(2\pi)^3}\frac{\delta_{ij}-\frac{k_ik_j}{\mathbf{k}^2+\lambda^2}}{2\sqrt{\mathbf{k}^2+\lambda^2}}\;\frac{1}{E-\frac{\mathbf{p}^2}{2m}-\sqrt{\mathbf{k}^2+\lambda^2}}\;\frac{1}{E-\frac{\mathbf{p}^2}{2m}}\;(-eA_0)\;\xi. \tag{13}$$

Here, E represents the on-shell energy $\mathbf{p}^2/2m$. Of course, in that limit, the propagator $1/(E-\mathbf{p}^2/2m)$ is divergent, which signals the need for a mass renormalization. In NRQED, we perform mass renormalization exactly as in QED, *i.e.* we start by keeping $E \neq \mathbf{p}^2/2m$ and subtract the mass counter-term:

$$-\frac{1}{2}\xi'^{\dagger} eA_0 (\frac{e}{m})^2 \frac{\mathbf{p}^2}{3} \int \frac{dk\ \mathbf{k}^2}{2\pi^2} \frac{2\mathbf{k}^2+3\lambda^3}{\mathbf{k}^2+\lambda^2} \frac{1}{2\sqrt{\mathbf{k}^2+\lambda^2}} \left(\frac{1}{E-\frac{\mathbf{p}^2}{2m}-\sqrt{\mathbf{k}^2+\lambda^2}} - \frac{1}{-\sqrt{\mathbf{k}^2+\lambda^2}}\right) \frac{1}{E-\frac{\mathbf{p}^2}{2m}}\ \xi. \tag{14}$$

Expanding the term in the parenthesis around $E-\frac{\mathbf{p}^2}{2m}$, we get a series which, by construction, starts at order $(E-\mathbf{p}^2/2m)^1$, which cancels the propagator $1/(E-\mathbf{p}^2/2m)$ in Eq.(13). One can then finally take the limit $E \to \mathbf{p}^2/2m$ with for result, for the sum of Figs.[10(i)] and [10(k)],

$$-\frac{1}{2}\xi'^{\dagger}\ eA_0\ \frac{\alpha}{3\pi m^2}(\mathbf{p}^2+\mathbf{p}'^2)\int dk\mathbf{k}^2 \frac{2\mathbf{k}^2+3\lambda^2}{\mathbf{k}^2+\lambda^2}\ \frac{1}{\sqrt{\mathbf{k}^2+\lambda^2}}\ \frac{-1}{\mathbf{k}^2+\lambda^2}\xi$$
$$= -\frac{8\alpha}{3\pi}\left[\ln(\frac{2\Lambda}{\lambda})-\frac{5}{6}\right]\left(\frac{-\xi'^{\dagger}eA_0\xi}{8m^2}(\mathbf{p}^2+\mathbf{p}'^2)\right). \tag{15}$$

Putting everything together, the complete right-hand side of Fig.[10] is equal to the sum of Eqs.(12) and (15):

$$\xi'^{\dagger}(-eA^0)\,\xi \quad + \quad \frac{e}{8m^2}\xi'^{\dagger}\,\mathbf{Q}^2 A^0 \xi\left[\delta_D + \frac{8\alpha}{3\pi}\left(\ln(\frac{2\Lambda}{\lambda})-\frac{5}{6}\right)\right]$$
$$- \quad \delta_S\,\frac{ie}{4m^2}\xi'^{\dagger}\,\boldsymbol{\sigma}\cdot(\mathbf{p}\,'\times\mathbf{p})A^0\,\xi \tag{16}$$

Now, by equating (11) and (16), we can evaluate δ_D and δ_S:

$$\delta_D = 1+\frac{\alpha}{\pi}\frac{8}{3}\left[\ln(\frac{m}{2\Lambda})+\frac{11}{24}\right]+2a_e+\mathcal{O}(\alpha^2) \tag{17}$$
$$\delta_S = 1+2a_e+\mathcal{O}(\alpha^2). \tag{18}$$

Notice that, since the relativistic kinetic vertex does not enter the matching, we also find[2]

$$\delta_R = 1+\mathcal{O}(\alpha^2). \tag{19}$$

We are now ready for the third and last step of the calculation, the computation of the bound state diagrams *per se*. Since only δ_D and δ_S receive an $\mathcal{O}(\alpha)$ correction, but not

[2]One might expect that δ_R be equal to one to all orders, since this interaction comes from Taylor expanding the relativistic expression for the energy, but this might not be so if the regulator (as is the case in this calculation) breaks Lorentz invariance.

δ_R, only Figs.[7(b)] and [7(c)] are needed for the $\mathcal{O}(\alpha^5)$ calculation. Let us now start with Fig.[7(b)].

$$\begin{aligned}
\Delta E_{7(b)} &= \delta_S \frac{-iZe^2}{4m^2}\int \frac{d^3p' d^3p}{(2\pi)^6}\Psi^*(\mathbf{p})\Big(\frac{\boldsymbol{\sigma}\cdot\mathbf{p}\,'\times\mathbf{p}}{(\mathbf{p}\,'-\mathbf{p})^2}\Big)\Psi(\mathbf{p}\,') \\
&= \delta_S\ \frac{Z\alpha}{2m^2} < \frac{\mathbf{s}\cdot\mathbf{L}}{r^3} > \\
&= \delta_S\ \frac{m(Z\alpha)^4}{4n^3(l+1/2)}\Big(\frac{\delta(j-(l+1/2))}{(l+1)} - \frac{\delta(j-(l-1/2))}{l}\Big)(1-\delta_{l,0}),
\end{aligned} \tag{20}$$

where $\Psi(\mathbf{p})$ is the Schrödinger wavefunction (including the electron spin[3] corresponding to the quantum numbers n, j and l.

In Eq.(20) we used

$$\int \frac{d^3p'}{(2\pi)^3} e^{i\mathbf{p}\,'\cdot\mathbf{r}\,'}\frac{\boldsymbol{\sigma}\cdot\mathbf{p}\times\mathbf{p}\,'}{\mathbf{p}'^2} = i\frac{\boldsymbol{\sigma}\cdot\mathbf{p}\times\mathbf{r}\,'}{4\pi r'^3}. \tag{21}$$

For the diagram of Fig.[7(c)], we find

$$\begin{aligned}
\Delta E_{7(c)} &= \int \frac{d^3p' d^3p}{(2\pi)^6}\Psi^*(\mathbf{p}\,')\Big(\delta_D\ \frac{e(\mathbf{p}\,'-\mathbf{p})^2}{8m_a^2}\ Ze\ \frac{1}{(\mathbf{p}\,'-\mathbf{p})^2}\Big)\Psi(\mathbf{p}) \\
&= \int \frac{d^3p' d^3p}{(2\pi)^6}\Psi^*(\mathbf{p}\,')\Psi(\mathbf{p}) \\
&= \delta_D\ \frac{Ze^2}{8m^2}|\Psi(0)|^2 = \delta_D\ \frac{m(Z\alpha)^4}{2n^3}\delta_{l,0}.
\end{aligned} \tag{22}$$

Using the counting rules, we also found that the diagram depicted in Fig.[8] would contribute to $\mathcal{O}(m\alpha^5)$. This diagram corresponds to the well-known Uehling potential and is found to be

$$\begin{aligned}
\Delta E_8 &= \int \frac{d^3p' d^3p}{(2\pi)^3}\Psi^*(\mathbf{p}\,')\Big(-e\ \frac{1}{(\mathbf{p}\,'-\mathbf{p})^2}\delta_{VP}\frac{-(\mathbf{p}\,'-\mathbf{p})^4\alpha}{15\pi m^2}\ \frac{1}{(\mathbf{p}\,'-\mathbf{p})^2}\ Ze\Big)\Psi(\mathbf{p}) \\
&= -\delta_{VP}Ze^2\frac{\alpha}{15\pi}\frac{1}{m^2}|\Psi(0)|^2 = -\delta_{VP}\frac{4\alpha}{15\pi}\frac{m(Z\alpha)^4}{n^3}\delta_{l,0}.
\end{aligned} \tag{23}$$

We finally turn our attention to the only remaining diagram, which is represented in Fig.[10]. The corresponding integral is (as shown in Ref.[2], in zeroth order of the multipole expansion we set $\mathbf{p}\,' = \mathbf{p}$ on the vertices):

$$\Delta E_8 = \int \frac{d^3k d^3p}{(2\pi)^6}\Psi^*(\mathbf{p})\ \frac{2ep_i}{2m}\frac{2ep_j}{2m}\frac{1}{2k}\frac{1}{E_n - \frac{\mathbf{p}^2}{2m} - k}(\delta_{ij} - \frac{k_i k_j}{\mathbf{k}^2})\ \Psi(\mathbf{p})$$

[3] In the non-recoil limit, the spin of the proton completely decouples from the problem.

$$= \frac{e^2}{2m^2(2\pi)^3}\int\frac{d^3p}{(2\pi)^3}\Psi^*(\mathbf{p})\int dk\ k d\Omega\frac{(\mathbf{p}^2-\frac{(\mathbf{p}\cdot\mathbf{k})^2}{\mathbf{k}^2})}{E_n-\frac{\mathbf{p}^2}{2m}-k}\Psi(\mathbf{p})$$
$$= \frac{2\alpha}{3\pi}\int\frac{d^3p}{(2\pi)^3}\int dk\,k\ \Psi^*(\mathbf{p})\ (\frac{\mathbf{p}^2/m^2}{E_n-\frac{\mathbf{p}^2}{2m}-k})\ \Psi(\mathbf{p}). \tag{24}$$

In a bound state, beyond tree level one must include an infinite number of Coulomb lines in the intermediate state. This can easily be seen from the counting rules, Eq.(8). Indeed, adding a Coulomb line will not change ζ because this increases both N_{top} and $\sum_i n_i$ by one, which has no overall effect. Because of this, one must use the Coulomb Green's function for the intermediate state. Using the bra and ket notation, Eq.(24) must then be replaced by the well-known expression:

$$\frac{2\alpha}{3\pi}\sum_{n'}\int dk\ k\ \frac{<n|\mathbf{v}_{op}|n'><n'|\mathbf{v}_{op}|n>}{E_n-E_{n'}-k}. \tag{25}$$

This part of the calculation is well known and is carried out in many texbooks (see for example Ref.[5]). The result is

$$\Delta E = m\frac{4\alpha}{3\pi}\frac{(Z\alpha)^4}{n^3}\begin{cases}\ln\frac{\Lambda}{<E_n>} & \text{if } l=0\\ \ln\frac{Z^2m\alpha^2}{2<E_n>} & \text{if } l\neq 0,\end{cases} \tag{26}$$

where $<E_n>$ is the Bethe logarithm which can be evaluated numerically [9]. Now, using Eqs.(17) and (18), we add the α^5 contributions from Eqs.(20) and(22) to Eqs.(23) and (26) to obtain

$$\Delta E = m\frac{4\alpha}{3\pi}\frac{(Z\alpha)^4}{n^3}\begin{cases} ln\frac{m}{2<E_{n,0}>}+\frac{19}{30} & \text{if } l=0\\ \ln\frac{Z^2m\alpha^2}{2<E_{n,l}>}+\frac{3}{8(2l+1)}(\frac{\delta(j-(l+1/2))}{(l+1)}-\frac{\delta(j-(l-1/2))}{l}) & \text{if } l\neq 0,\end{cases} \tag{27}$$

which is the well-known Lamb shift.

2 Conclusion

We have calculated the complete $\mathcal{O}(m\alpha^5)$ non-recoil corrections to the hydrogen energy levels, also referred to as the Lamb shift. The superiority of NRQED over the traditional approaches is twofold. Firstly, the calculation of the bound state diagrams is greatly simplified because the use of an effective field theory permits to disentangle the contributions from low and high momenta and only QED *scattering* diagrams need to be evaluated. Secondly, the NRQED calculation is *systematic* in the sense that simple counting rules can be used to isolate the diagrams contributing to a given order in α, which is not possible in traditional approaches.

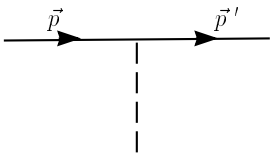

Coulomb Vertex

q

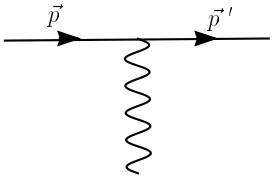

Dipole Vertex

$$-\frac{q}{2m}(\vec{p}\,' + \vec{p})$$

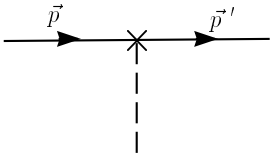

Darwin Vertex

$$\delta_D \ \frac{-q}{8m^2}(\vec{p} - \vec{p}\,')^2$$

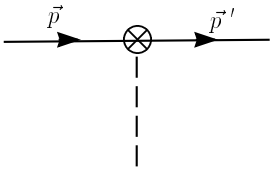

Spin-Orbit Vertex

$$\delta_S \ \frac{iq}{4m^2}(\vec{p}\,' \times \vec{p}) \cdot \vec{\sigma}$$

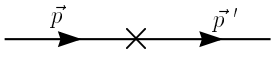

Relativistic Kinetic Vertex

$$-\frac{\vec{p}^{\,4}}{8m^3}(2\pi)^3\delta^3(\vec{p}\,' - \vec{p})$$

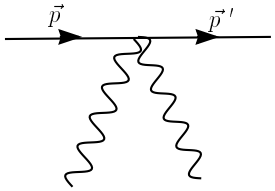

Seagull Vertex

$$q^2\frac{\delta^{ij}}{2m}$$

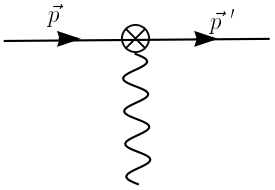

Fermi Vertex

$$\delta_F \ \frac{iq}{2m}(\vec{p}\,' - \vec{p}) \times \vec{\sigma}$$

Figure 1: NRQED Vertices

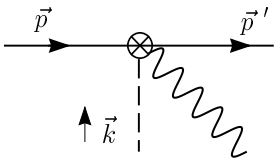

Spin-Seagull Vertex

$$\delta_S \ \frac{iq^2}{4m^2}\vec{k}\times\vec{\sigma}$$

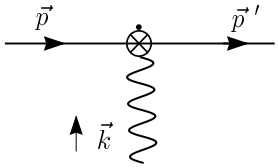

Time Derivative Vertex

$$\delta_S \ \frac{-iq}{8m^2}k^0(\vec{p}\,'+\vec{p})\times\vec{\sigma}$$

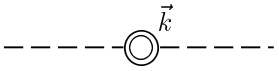

Coulomb Vacuum Polarization Vertex

$$\delta_{VP} \ \frac{-\alpha}{15\pi} \ \frac{\vec{k}^4}{m^2}$$

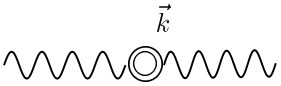

Transverse Vacuum Polarization Vertex

$$\delta_{VP} \ \frac{\alpha}{15\pi} \ \frac{\vec{k}^4}{m^2}\Big(\delta_{ij}-\frac{k_ik_j}{\vec{k}^2}\Big)$$

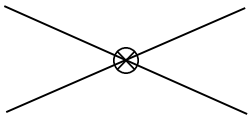

Anihilation Vertex

$$\delta_{4-F} \ \frac{q^2}{4m}\vec{S}^2$$

NRQED Vertices (continued)

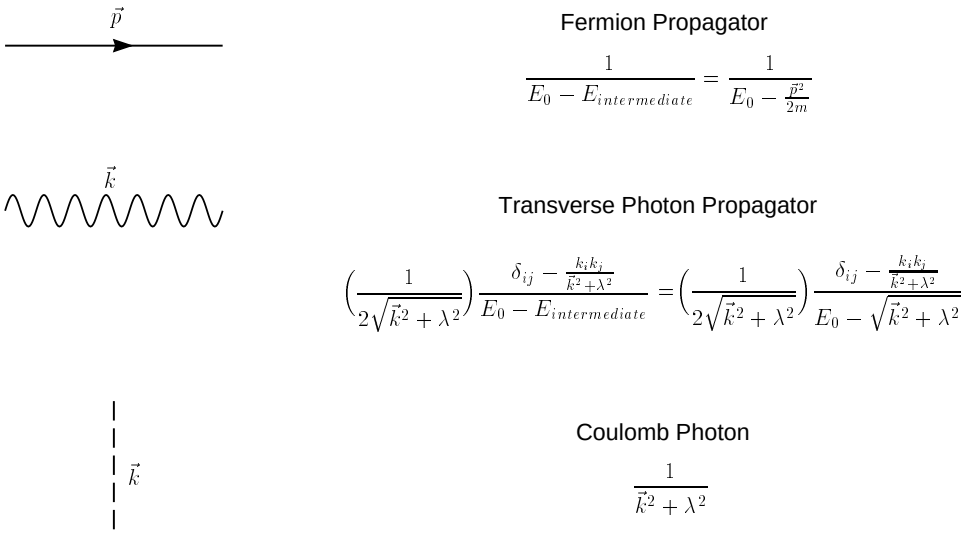

Figure 2: NRQED Propagator

.

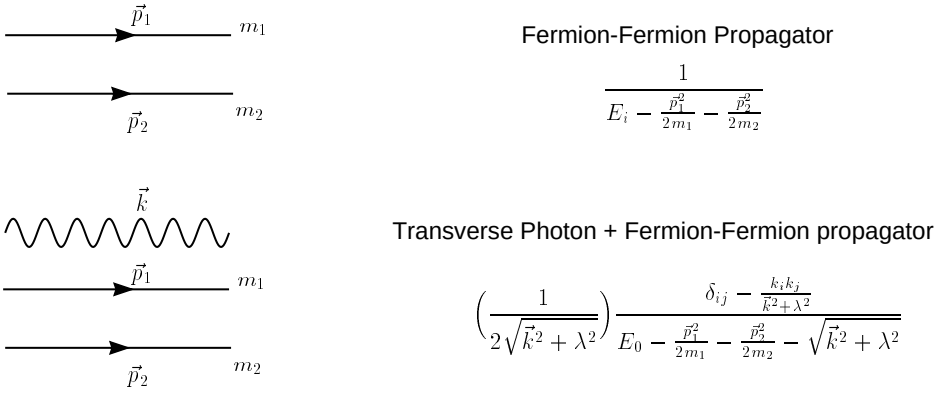

Figure 3: Time-ordered propagators for two fermions plus one transverse photon.

.

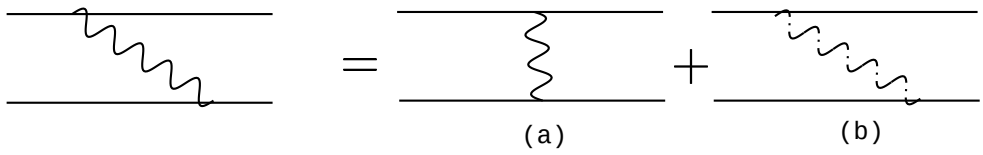

Figure 4:

.

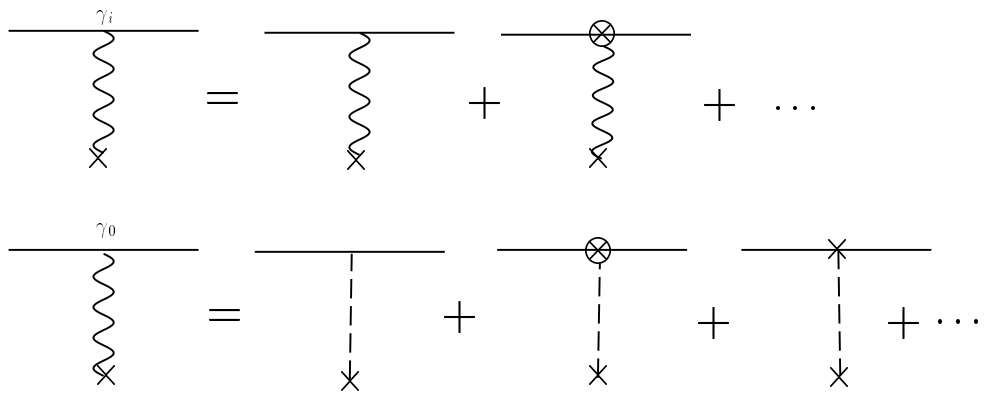

Figure 5:

.

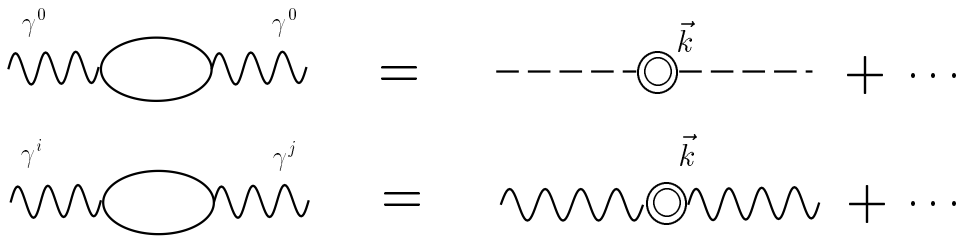

Figure 6:

.

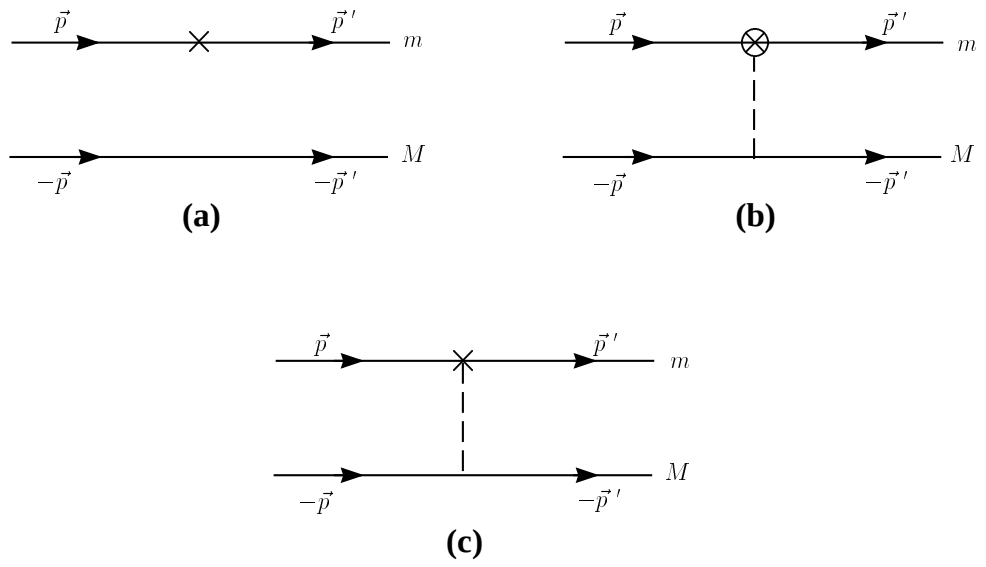

Figure 7:

.

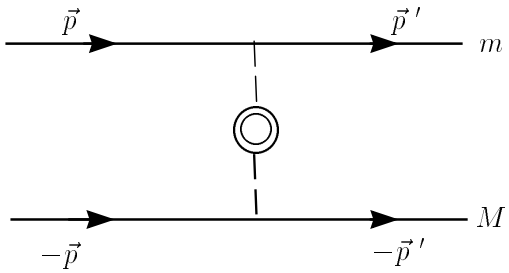

Figure 8:

.

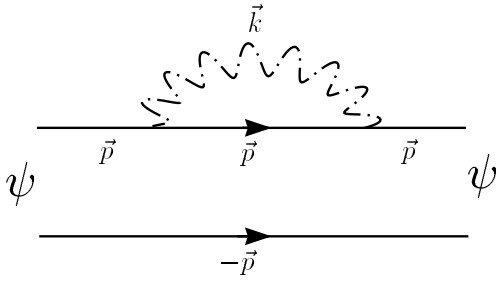

Figure 9:

.

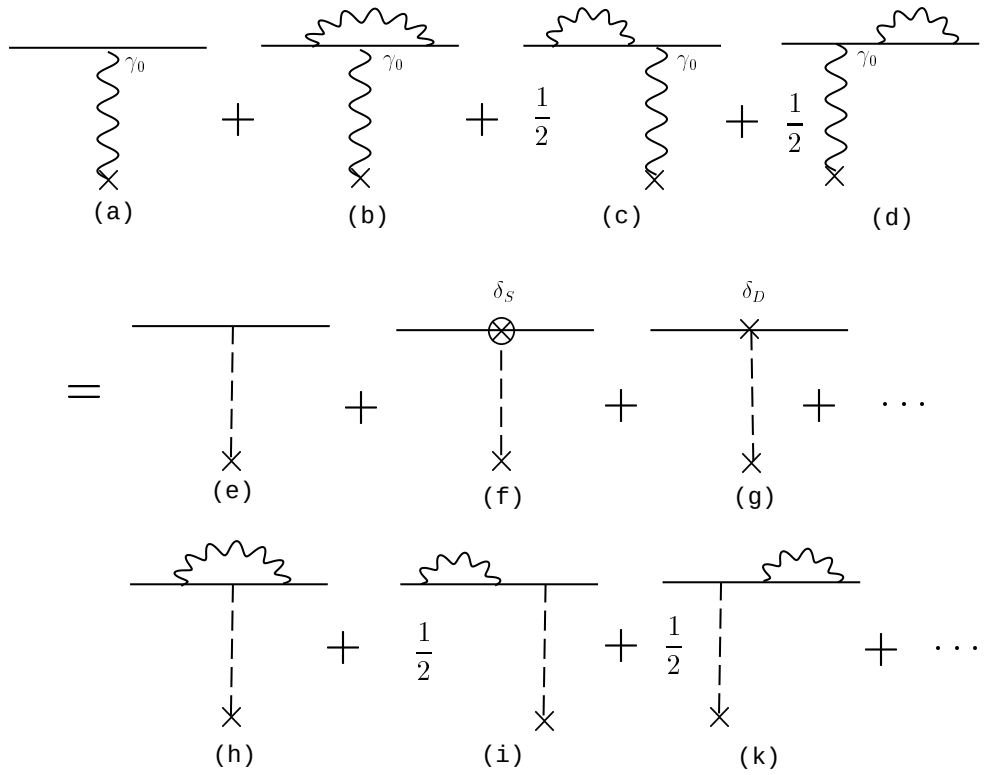
γ_0
γ_0
$\frac{1}{2}$
γ_0
$\frac{1}{2}$
γ_0
(a)
(b)
(c)
(d)
=
δ_S
δ_D
(e)
(f)
(g)
$\frac{1}{2}$
$\frac{1}{2}$
(h)
(i)
(k)

Figure 10:

.

References

[1] W.E. Caswell and G.P. Lepage, Phys. Rev. **A20**, 36 (1979).

[2] P. Labelle, hep-ph/9608491.

[3] P. Labelle, G. P. Lepage, and U. Magnea, Phys. Rev. Lett. **72**, 2006 (1994).

[4] P. Labelle, Ph.D. Thesis, Cornell University, January (1994).

[5] C.Itzykson and Zuber, Quantum Field Theory, McGraw-Hill,1980.

[6] P. Labelle, "NRQED in bound states: applying renormalization to an effective field theory", proceedings of the fourteenth MRST Meeting, P.J. O'Donnell ed., University of Toronto, 1992, hep-ph/9209266.

[7] T. Kinoshita, M. Nio, Phys. Rev. **D**53, 4909, 1996.

[8] P.Labelle, S M Zebarjad, work in preparation.

[9] J.R. Sapirstein and D.R. Yennie in *Quantum Electrodynamics*, ed. by T. Kinoshita (World Scientific, Singapore, 1990).